Environ. Sci. Technol. **2002**, *36,* 21−29

Assessing the Combined Roles of Natural Organic Matter and Black Carbon as Sorbents in Sediments

AMYMARIE ACCARDI-DEY AND
PHILIP M. GSCHWEND*
*Ralph M. Parsons Laboratory, MIT 48-415,
Department of Civil and Environmental Engineering,
Massachusetts Institute of Technology,
Cambridge, Massachusetts 02139*

We hypothesized that two mechanisms, *ab*sorption into natural organic matter and *ad*sorption onto combustion-derived black carbon (BC), act in parallel to bind polycyclic aromatic hydrocarbons (PAHs) to Boston Harbor sediments. To focus on BC-adsorption, we removed the non-BC fraction by combusting near shore sediments at 375 °C for 24 h under air, leaving ca. 16% of the reduced carbon. The isotherm for pyrene sorption onto our combusted sediment was nonlinear with a Freundlich exponent of 0.62 ± 0.12 and a BC-normalized distribution coefficient (μg/kg$_{\rm BC}$)/(μg/L)^n of $10^{6.25\pm0.14}$. Pyrene sorption to untreated sediment was reasonably estimated using $K_d = f_{oc}\, 10^{4.7} + f_{BC}\, 10^{6.25}\, C_w^{(0.62-1)}$ where f_{oc} was the non-BC organic carbon content, $10^{4.7}$ was the organic carbon-normalized absorption coefficient for pyrene (L/kg$_{\rm oc}$), f_{BC} was the BC content, and C_w was the dissolved pyrene concentration (μg/L). C/H/N ratios indicated that our environmental BC differed substantially from NIST diesel soot, possibly due to inclusion of larger BC particles from near source atmospheric fallout and urban runoff. The impact of BC on total PAH sorption may explain reports of nonlinear isotherms, K_{oc} values for PAHs that exceed their respective K_{ow} values, and discrepancies in bioavailability between planar and nonplanar sorbates.

Introduction

Sorption is a key process controlling the fate of organic pollutants in the environment. It can limit the degradation of pollutants as well as influence the rate and extent that bioaccumulation occurs. A quantitative understanding of sorption is necessary to evaluate the hazards that pollutants pose.

Laboratory studies since the late 1970s have indicated that nonionic organic compounds partition into the natural organic matter of sediments and soils (*1*, *2*). This conceptualization yielded a solid−water distribution coefficient (K_d, L/kg$_{\rm solid}$):

$$K_d = f_{oc}\, K_{oc} \tag{1}$$

where f_{oc} is the weight fraction of organic carbon (OC) in the solid phase, which serves as a metric of the organic matter content, and K_{oc} is the OC-normalized distribution coefficient for the compound of interest (L/kg$_{\rm oc}$). However, investigators in the early 1990s noted that this linear relationship failed to characterize the equilibrium sorption of nonionic organic compounds in some laboratory studies (*3*). To account for these observations, Weber et al. hypothesized that organic matter consists of a heterogeneous mix of sorbents, for example, “soft” and “hard” carbon. Additional research on other processes influenced by sorption, such as bioremediation and bioaccumulation, suggested that some phenomenon “sequestered” chemicals or limited their accessibility (*4*−*8*). One explanation for these observations was that a strong sorbent in addition to OC was present in the sediments and soils (*9*−*12*).

Meanwhile, investigators have observed in the field that polycyclic aromatic hydrocarbons (PAHs) sorbed to sediments more than predicted by the $f_{oc}K_{oc}$ model (*13*−*19*). These researchers and others recognized that PAHs, derived from pyrogenic sources (*20*, *21*), co-occur in soils and sediments with soot, chars, and other carbonaceous particles, collectively called “black carbon” (BC) in this paper. Gustafsson et al. and Gustafsson and Gschwend proposed that the BC fraction in sediments and soils acted like activated carbon accounting for the high sorption affinities for PAHs (*10*, *22*). In support of this contention, Bucheli and Gustafsson demonstrated that PAHs exhibit high distribution coefficients and nonlinear isotherms for sorption onto NIST diesel particulate matter (soot, SRM 1650) (*23*).

Here, we propose that BC and OC act in parallel to sorb organic compounds from the water. The BC in sediments would act as an *adsorbent* interacting with organic molecules of planar structure (*24*), and Freundlich isotherms, reported widely for activated carbons (*25*−*27*) and diesel soot (*23*), should characterize these adsorbent interactions. Simultaneously, the OC would serve as an *absorbent* that operates as described by Chiou et al. and Karickhoff (*1*, *2*). Hence at equilibrium, the sorbed PAH concentration is hypothesized to depend on the dissolved PAH concentration according to:

$$C_s = f_{oc}K_{oc}C_w + f_{BC}K_{BC}{C_w}^n \tag{2}$$

where C_s is the sorbed concentration (μg/kg$_{\rm solid}$), C_w is the truly dissolved concentration (μg/L), f_{BC} is the weight fraction of BC in the solid phase, K_{BC} is the BC-normalized distribution coefficient (μg/kg$_{\rm BC}$)/(μg/L)$^{\rm n}$, and n is the Freundlich exponent appropriate for each PAH-BC combination of interest. Given this formulation, the solid−water distribution coefficients should take the form:

$$K_d = f_{oc}K_{oc} + f_{BC}K_{BC}{C_w}^{n-1} \tag{3}$$

Observations reported by other investigators appear likely to fit such a model (*28*−*32*).

In this study, we assessed the $f_{oc}K_{oc}$ and the $f_{BC}K_{BC}{C_w}^{n-1}$ contributions to the overall sorption of a representative PAH, pyrene, interacting with sediments from Boston Harbor, MA. To this end, we investigated pyrene sorption to both untreated sediments and precombusted sediments (at 375 °C for 24 h under air (*10*)). The sediments were characterized with respect to both their elemental mole ratios and their f_{oc} and f_{BC} contents. Then, the combusted sediments were used to determine the sorption isotherm (K_{BC} and n) for pyrene interacting with environmental BC as this material occurs in the Boston Harbor. Our work indicated that (1) BC is the dominant sorbent for pyrene at our sites, (2*)* sorption of pyrene onto untreated sediment involves the sum of partitioning into OC plus adsorption onto BC, and (3) the equilibrium distribution coefficient for BC in the Boston

---

* Corresponding author phone: (617)253-1638; fax: (617)253-7395; e-mail: pmgschwe@mit.edu.

10.1021/es010953c CCC: $22.00

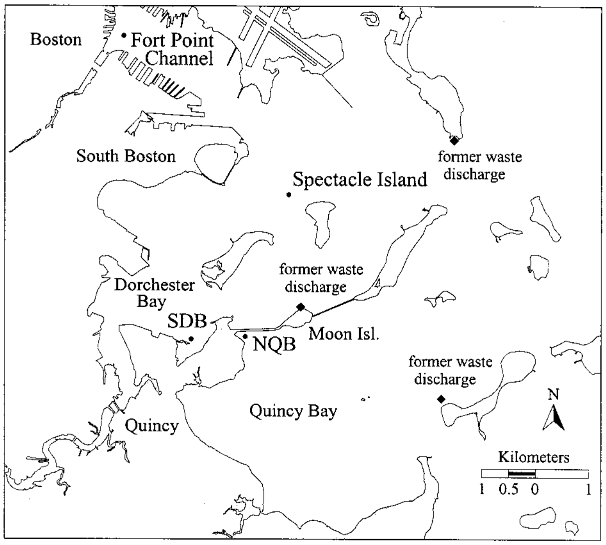

FIGURE 1. Map of Boston Harbor, MA showing the locations of SDB (south Dorchester Bay, 42°18.0′ N, 71°1.8′ W) and NQB (north Quincy Bay, 42°18.1′ N, 71°1.0′ W) along with two other sites previously examined by McGroddy and Farrington (*16*) and Gustafsson et al. (*10*): Fort Point Channel (42°21′22″ N, 71°02′41″ W) and Spectacle Island (42°19′46″ N, 70°59′34″ W). The map also shows the approximate locations of former waste discharge outlets.

Harbor is lower than the corresponding distribution coefficient for NIST diesel soot.

Methods

Sediments. Grab samples of surface sediment were collected from littoral sites in Boston Harbor at south Dorchester Bay (SDB) and north Quincy Bay (NQB) near Quincy, MA in December 1999. Subsamples from box cores taken in 1990 (*16*) were also gathered from sites near Fort Point Channel (FPC) and Spectacle Island (SI; Figure 1). Previous studies (*33, 34*) have shown that these bays, and the adjacent Moon Island region, are polluted from a waste discharge outlet with PAH concentrations in the sediment exceeding 20 000 ng ΣPAHs/gdw. For each site, a 5 g sample was dried (75 °C), and coarse grains were manually removed. The remaining sediment was then ground with a mortar and pestle and sieved through a 425 μm aperture, ultimately removing 30% of the sediment by weight. A 450 mg subsample was then combusted in a Sybron F-A1730 Thermolyne muffle furnace (Dubuque, IA) under air for 24 h at 375 °C. This method oxidizes labile organic matter but retains a BC fraction in the sediment (*10, 35*).

A Perkin-Elmer 2400 CHN Elemental Analyzer (Norwalk, CT) was used to determine the carbon weight percent and elemental mole ratios for both the untreated and combusted sediments. Sediment samples were not acidified to remove carbonate solids because test samples showed that the carbon added during the acidification method was greater than the amount of BC present in the sediment. In the untreated sediment, the carbon weight percent was assumed to include both the OC and BC, whereas the carbon in the combusted sediment was operationally defined as the BC fraction. The OC in the untreated sediments was obtained by subtracting the two carbon weight percents. NIST diesel particulate matter (soot, SRM 1650) was also combusted and analyzed on the CHN Elemental Analyzer. The CHN response factors were determined using acetanilide standards (Elemental Microanalysis, Manchester, MA) and were monitored after every six samples to check for reproducibility. The carbon and nitrogen response factors were more stable and reproducible (±0.03% for carbon and ±1% for nitrogen with 1500 μg acetanilide) than the hydrogen response factor (±8%). Elemental weight percents were accepted only when standard acetanilide samples were within ±0.3 wt % of the known acetanilide values. The signal-to-noise ratio was >4:1 for the combusted samples and >10:1 for untreated samples with a detection limit of 8.9 ± 0.6 μg carbon. (The signal-to-noise ratio corresponds to the number of CHN electronic counts with a sample compared to the number of counts without a sample.) Blanks were run after samples to verify that combustion was complete. All reported CHN errors represent ±1 standard deviation.

PAH Extraction. Approximately 5 g of untreated wet sediment were spiked with deuterated PAH recovery standards: d_{10}-acenaphthene, d_{10}-phenanthrene, d_{14}-p-terphenyl, d_{12}-benz[*a*]anthracene, and d_{12}-perylene (*10*). The sediment was Soxhlet extracted for 24 h using a 9:1 mixture of CH_2Cl_2:CH_3OH. Anhydrous Na_2SO_4 was used to precipitate residual water in the extract, and activated copper was used to precipitate elemental sulfur. The extract was concentrated and exchanged into hexane using a Kuderna-Danish apparatus and N_2-blow down techniques. The concentrate was fractionated on a fully activated silica gel column (EM Science, 100−200 mesh, 16:1 height to width). PAH quantification was performed on a JEOL GCmate gas chromatograph-mass spectrometer, equipped with a Hewlett-Packard 6890 gas chromatograph. Extracts were injected splitless and separated on a 30 m × 0.32 mm DB-5 (0.25 μm film thickness) fused-silica capillary column (J&W Scientific, Inc.) The temperature program began with a 20 °C/min ramp from 70 °C to 180 °C, followed by 6 °C/min from 180 °C to 300 °C. The injector and transfer zone temperatures were 280 °C, and the MS source temperature was 250 °C. Electronic pressure control maintained the He flow rate at 2 mL/min. The response factors, determined daily with a three-point calibration curve, had a variability of ±7%. Procedural blanks were analyzed concurrently with the samples. Blanks were <0.6 pg/μL-injection corresponding to a signal-to-noise ratio >500:1 for the PAHs reported. Using the methodology described above, our laboratory found 81 ± 32% (±2σ) of the certified concentrations of several PAHs reported for NIST NY/NJ waterway sediment (SRM 1944) and NIST marine sediment (SRM 1941a).

Sorption. Sorption experiments were conducted in precombusted, 100-mL volumetric flasks with untreated or combusted sediment (10−200 mg) and varying initial concentrations of pyrene (2−21 μg/L, Aldrich Chemical Co., Milwaukee, WI). Each sorption experiment included a control flask that contained the initial dissolved pyrene concentration, another control flask that contained only sediment and water (18 mΩ, low-carbon water produced using an Aries Vaponic system, Rockland, MA), and an experimental flask that contained both sediment and dissolved pyrene. All flasks were closed with glass stoppers, covered to avoid the photodegradation of pyrene, and tumbled once every 3 s for a minimum of 1 month. Losses of dissolved pyrene in control flasks were <5% over the duration of the experiment.

A Perkin-Elmer LS50B Luminescence Spectrofluorometer (Buckinghamshire, England) was used to monitor the pyrene in solution in the flasks. Before sampling, the flasks stood overnight undisturbed to allow particles to settle. A Stokes calculation revealed that a particle with a radius of 1 μm will settle to the bottom of a 100 mL volumetric flask within 12 h (overnight) at $T = 24$ °C assuming a density of 2.5 g/cm^3. Aliquots were transferred to a Starna quartz cell (1 cm path length; Atascadero, CA) for fluorescence analysis at 272.5 nm (excitation wavelength) and were then returned to their respective flasks. The background signals from the control flasks (containing sediment and water) were subtracted from the pyrene signals from the experimental flask. Fluorescence signals were quantified by synchronous scans, which were performed with a $\Delta\lambda$ of 100 nm, an entrance slit of 2.5 nm, an exit slit of 5.0 nm, and a scan speed of 240 nm/min (*36*). The detection limit of the spectrofluorometer with these parameters was 0.27 μg pyrene/L (signal-to-noise of 3:1) with a 13% instrumental error. This instrumental error decreased to 4% when pyrene concentrations were >1 μg/L. We designed our experiments to have final dissolved pyrene concentrations on the order of 0.5 μg/L to 10 μg/L because of the limitations of the LS50B spectrofluorometer. This concentration range was greater than typical ambient concentrations, but it allowed for precise sorption observations with triplicate experiments varying <10%. All reported sorption parameters and errors (representing ±1 standard deviation) were generated using SigmaPlot version 4 (Scientific Graphing Software, SPSS Inc.). Errors were propagated for derived parameters following the equations listed in Harris (*37*).

Kinetics. Using SDB sediment, kinetic experiments were performed in a manner similar to the sorption experiments described above. However, tubes were spiked with 1 mM sodium azide (Fluka Chemika, Switzerland) to inhibit microbial growth and activity. Before analyzing these solutions with the spectrofluorometer, the tubes were centrifuged at 1100*g* for 8 min. After analysis, the tubes were returned to the tumbler within 1 h. Test samples showed no difference in the fluorescence intensity between centrifuging and allowing particles to settle overnight.

Quenching. Additional experiments were conducted to determine if the organic carbon desorbing from the sediments was affecting the dissolved pyrene fluorescence by quenching or inner filter effects (*38*−*40*). Supernatants were obtained from a control flask of sediment and water centrifuged at 1100*g* for 8 min. The absorbance values of these supernatants were measured using 272.4 nm (excitation) and 372.4 nm (emission) wavelengths on a Beckman DU640 Spectrophotometer (Fullerton, CA) in a Uvonic quartz cuvette (1 cm path length; Plainview, NY) to investigate inner filter effects. Then, successive 100 μL spikes of pyrene were added to the supernatant and a corresponding flask containing only Aries Vaponic water. Fluorescence intensities between successive spikes in the two flasks were compared to determine if fluorescence quenching was present.

Influence of Pretreatment Temperature. Since the Thermolyne muffle furnace operated with a slow-response thermocouple control (Furnatrol 133, Sybron Corp), variations in the combustion temperature could affect the quantity and quality of BC retained. A typical temperature cycle involved a ramp from 364 °C ± 1 °C to 375 °C ± 1 °C at 2 °C/min for 5 min followed by a cool at 1 °C/min for 10 min. To assess the effect of this temperature variability on sorption, sediments were also combusted in a Fisher Scientific IsoTemp programmable muffle furnace at the Woods Hole Oceanographic Institution (WHOI) at three different temperatures: 365 °C, 375 °C, and 385 °C. The temperature program included a ramp at 15 °C/min to 300 °C, hold for 5 min, a second ramp at 5 °C/min to the designated combustion temperature, and a hold for 24 h. Sorption experiments were then conducted on these sediments to deduce the sensitivity of our results within this temperature range.

Results and Discussion

PAH Composition. The mix of PAHs in the sediment suggested that high-temperature pyrolysis was the dominant source of the PAHs and BC deposited at SDB and NQB. For both SDB and NQB, the phenanthrene/Σmethylphenanthrenes ratio was 3, and the fluoranthene/pyrene ratio was 1. The phenanthrene/anthracene ratio was 6 at NQB and 4 at SDB. All these ratios are consistent with a high-temperature pyrogenic source, rather than a petrogenic source (*20*, *21*, *41*). In addition, the dimethylphenanthrenes (DMP) distribution, and especially the ratio of 1,7-DMP/2,6-DMP, indicated the predominance of a fossil fuel pyrogenic source as opposed to a wood burning source (*42*−*44*). In light of the urban surroundings of these bays, such pyrogenic inputs of PAHs and BC are likely derived from atmospheric fallout of BC particles (*45*), roadway runoff (*46*), and local combined sewer overflow sites.

TABLE 1. Results from CHN Elemental Analysis

	wt % carbon	C/H mole ratio	C/N mole ratio
South Dorchester Bay			
untreated sediment (OC+BC)	1.46 ± 0.13^{a}	0.7 ± 0.3^{c}	16 ± 1^{c}
combusted sediment (BC)	0.26 ± 0.07^{a}	0.7 ± 0.7^{c}	15 ± 4^{c}
North Quincy Bay			
untreated sediment (OC+BC)	3.68 ± 0.64^{a}	0.9 ± 0.3^{d}	16 ± 2^{d}
combusted sediment (BC)	0.60 ± 0.07^{a}	0.8 ± 0.1^{d}	17 ± 2^{d}
NIST Diesel Soot			
combusted soot	86.0 ± 1.60^{b}	11 ± 1^{d}	60 ± 3^{d}

[a] Weight percent (mean ± 1σ) equals total grams of elemental carbon per gram of dried sediment. [b] Weight percent (mean ± 1σ) equals total grams of elemental carbon per gram of NIST diesel soot (SRM 1650). [c] Acetanilide weight percents (mean ± 1σ): carbon ranged from 70.81 ± 0.01 to 71.29 ± 0.04, hydrogen ranged from 6.43 ± 0.24 to 6.99 ± 1.7, and nitrogen ranged from 10.32 ± 0.01 to 10.51 ± 0.08. [d] Acetanilide weight percents (mean ± 1σ): carbon ranged from 71.01 ± 0.02 to 71.03 ± 0.01, hydrogen ranged from 6.34 ± 0.43 to 8.37 ± 4.01, and nitrogen ranged from 10.36 ± 0.02 to 10.44 ± 0.05. C/H molar ratios are not reported when hydrogen weight percents exceeded 7.0 wt %.

CHN Elemental Analysis. The OC weight percent of untreated sediment from SDB was 1.2 ± 0.15% ($N = 10$) with a C/H/N mole ratio of 1/0.7 ± 0.3/16 ± 1 (Table 1). The untreated sediment from NQB had a substantially larger OC weight percent of 3.1 ± 0.64% ($N = 7$) but a similar C/H/N mole ratio of 1/ 0.9 ± 0.3/16 ± 2. After removing the labile OC by thermal oxidation, the BC weight percent in SDB sediment was 0.26 ± 0.07% ($N = 12$) with a C/H/N mole ratio of 1/0.7 ± 0.7/15 ± 4. The BC weight percent in the NQB sediment was 0.60 ± 0.07% ($N = 6$) with a C/H/N mole ratio of 1/0.8 ± 0.1/17 ± 2. For comparison, the elemental mole ratio for combusted NIST diesel soot was 1/11 ± 1/60 ± 3 ($N = 4$).

The BC weight percents for SDB and NQB were similar to those reported previously for two other stations in Boston Harbor: 0.66 ± 0.08% at FPC (7−9 cm) and 0.27 ± 0.04% at SI (0−2 cm) (*47*). However, the BC weight percents contributed a larger fraction of the total sedimentary reduced carbon (BC/(BC + OC)) at SDB and NQB than either FPC or SI. For example, our observations showed that at SDB and NQB, 16−18% of the total carbon was BC as opposed to 9−13% at the other Boston Harbor sites examined by Gustafsson and Gschwend (*47*). The higher BC/(BC + OC) ratios in the southern part of Boston Harbor may indicate that BC was less affected by postdepositional processes than OC in these littoral sediments, since BC is known as a recalcitrant material (*48*). Recently, Middelburg et al. investigated the postdepositional affects on BC in a 140 kyr-turbidite from the northwestern African margin. After 10−20 kyr of exposure to oxic pelagic conditions, only 36% of the BC was degraded in the turbidite (comparing the BC content in the upper oxidized section with the lower reduced section) (*49*). Based on these findings, weathering and postdepositional processes probably did not affect the BC characteristics in Boston Harbor since the sediment was only a few decades old.

The C/H and C/N ratios in the combusted sediments from SDB and NQB (Table 1) suggested that the BC deposited at these sites was not exclusively composed of the submicron soot particles typified by NIST diesel soot. Such submicron soot particles, which have a C/H mole ratio near 10 and C/N near 60 (Table 1 (*50−53*)), are likely transported farther offshore before settling out of the atmosphere (*54*). For example, Windsor and Hites estimated that the submicron soot particles generated in the Boston Metropolitan area had a residence time of 4 days and were transported an average over 1000 km offshore before settling (*45*). Conversely, larger (ca. 10 μm) BC particles would settle near their source and would accumulate in Boston Harbor from roadway runoff and sewer overflows. Rockne et al. also showed that C/H mole ratios varied among BC particles (*53*). They observed that while submicron soot particles generated in a flame had C/H ratios of 7.1 ± 0.4, the 10 μm BC particles collected from marine vessels and buses had C/H ratios of 0.72 ± 0.04 and 1.1 ± 0.06, respectively. Thus, our C/H data from combusted sediments (C/H ratios ranging from 0.4 to 1.5, Table 1) indicated that near shore BC might not be entirely submicron soot but rather a collection of larger combustion-derived BC particles. Furthermore, the similar C/H mole ratios for our combusted sediment and the BC particles reported by Rockne et al. suggest that our thermal oxidation method did not affect the surface chemistry of the BC in the sediment. Since BC forms at high temperatures (>1000 °C) in the absence of oxygen, exposure to 375 °C for 24 h in the presence of oxygen may have minimal surface effects, but further work is necessary to confirm this assumption.

While the C/N ratios reported here (C/N ratios ranging from 14 to 18, Table 1) were not corrected for the inorganic nitrogen potentially present in the sediment (*55*), our ratios suggest that the BC included more nitrogenous functionality than typically represented in chemical models of soot. Such models conceptualize soot as a super-PAH with occasional oxygen functional groups and alkyl chains (*56*)—nitrogen is not included in these models. However, if soot forms from the radical condensation of hydrocarbons (*57−59*), then nitrogenous radicals, such as NO_x species also produced during combustion, could also condense with these radical hydrocarbons. Roadway tunnel studies of diesel and gasoline exhaust have reported nitro-PAHs compounds in both the solid and gas phase (*60, 61*). In addition, Kozin et al. have also measured heterocyclic PAH in sediments of lakes and rivers (*62*). Hence, environmental BC might exhibit some nitrogen-derived functionality that could affect the sorption of H-bonding sorbates.

Sorption Method Checks. Kinetic experiments showed that the dissolved pyrene concentrations approached equilibrium with a half-life on the order of hours for the untreated SDB sediment (Figure 2). Interestingly, the combusted sediment from the same site approached equilibrium more slowly with a half-life of approximately 1 day. To ensure that pyrene reached equilibrium in our sorption experiments, they were conducted for over a month.

Within the sensitivity limits of the spectrofluorometer, pyrene fluorescence in the experimental supernatants was not quenched by dissolved organic carbon (DOC). Successive spikes of pyrene gave statistically indistinguishable incremental increases in fluorescence for the control solution, the supernatant from combusted sediment, and the supernatant from untreated sediment. Fluorescence measurements were also not affected by inner filter effects since the absorbance values at 272.4 and 372.4 nm were <0.002 for the supernatants. The absence of quenching and inner filter effects in our experiments was probably due to the low concentration of desorbed organic matter in the samples. Since the OC fraction at SDB was 0.012, the maximum concentration of carbon that could desorb from 50 mg of untreated sediment was 6×10^{-6} kg_{DOC}/L. These low DOC concentrations would not sorb a significant fraction of the dissolved pyrene assuming a pyrene-DOC distribution coefficient near 3×10^4 L/kg_{DOC} (*63−65*).

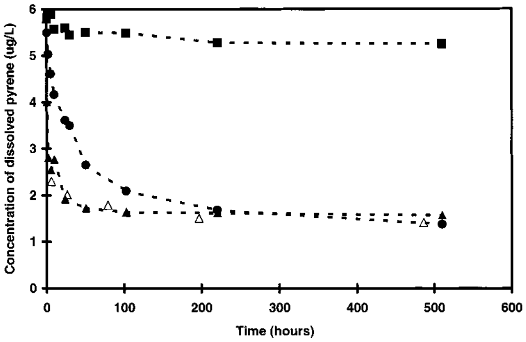

FIGURE 2. Kinetics experiment showing the loss of dissolved pyrene (μg/L) over time (hours) with (a) no sediment present (squares), (b) 40.0 mg of SDB combusted sediments (375 °C for 24 h under air) added to 0.049 L of solution (circles), and (c) replicate experiments using 40.0 mg of SDB untreated sediment added to both 0.049 L of solution (filled triangles) and 0.050 L of solution (open triangles). Each point is the average of four fluorescence measurements. The error associated with the dissolved pyrene concentrations in the control was ±4% and increased to ±8 to ±12% in the experimental flasks.

Pyrene Sorption. We observed between 20 and 90% loss of dissolved pyrene due to sorption in experiments using both untreated and combusted sediments from SDB and NQB (Table 2). The fraction of dissolved pyrene remaining in the water (f_w) after equilibrating with various sediments yielded a single sediment−water distribution coefficient (K_d, L/kg_{sed}) via:

$$K_d = \frac{(1 - f_w)}{f_w r_{sw}} \tag{4}$$

where r_{sw} is the ratio of sediment-to-water (kg_{sed}/L). Pyrene sorption for both the untreated and combusted sediments exhibited an average log K_d of 3.50 ± 0.20 for SDB (Figure 3a and Table 2) and an average log K_d of 3.72 ± 0.17 for NQB (Figure 3b and Table 2). In general, the data were slightly above average at concentrations lower than 2 μg/L and slightly below average at concentrations greater than 8 μg/L. Statistically, the slope for the untreated sediment in Figure 3a was −0.03 ± 0.01 with a R^2 of 0.62, and the slope for the combusted sediment in Figure 3a was −0.04 ± 0.02 with a R^2 of 0.52. These values were likely different from zero suggesting that the K_d values were dependent on the dissolved pyrene concentrations.

Influence of Combustion Temperature. Experiments involving SDB sediment combusted in a programmable oven at WHOI showed that pyrene sorption was sensitive to the pretreatment combustion temperature. Over the range of temperatures tested, the log K_d values decreased from 3.42 ± 0.05 for the 365 °C combusted sediment to 3.14 ± 0.08 for the 385 °C combusted sediment (Table 3). CHN analysis of these sediments showed that the BC weight percents also decreased from 0.22 ± 0.03 in the 365 °C combusted sediment to 0.15 ± 0.03 in for the 385 °C combusted sediment. In other words, the distribution coefficient decreased by a factor of 2 with increasing pretreatment temperatures, which corresponded to a 30% decline in the surviving f_{BC}.

These results indicated two caveats to our sorption data. First, because our Thermolyne muffle furnace operated with a slow-response thermocouple control, experimental imprecision was introduced when preparing the combusted sediment. While the carbon weight percent was tested after most burns, the assumption that the BC fraction in all the combusted sediment was uniform may not hold. Therefore, we believe that the log K_d values reported have ≤ 0.2 log units of error associated with imprecision in the combustion

TABLE 2. Summary of Sorption Experiments (Corresponds to Figure 3a,b)[a]

sorbent (mg)	volume (L)	initial concn (μg pyrene/L)	percent loss of dissolved pyrene	log K_d (L/kg)
		Untreated Sediment − South Dorchester Bay		
11.4	0.106	9.23	20.4	3.37
20.0	0.104	9.88	38.4	3.51
20.1	0.101	9.23	43.6	3.59
39.3	0.050	4.15	78.1	3.65
40.0	0.050	5.25	70.3	3.47
40.0	0.049	5.25	73.0	3.52
56.2	0.094	2.15	76.7	3.74
60.7	0.106	9.23	67.4	3.56
101.4	0.090	21.1	78.8	3.52
199.0	0.081	21.1	88.3	3.49
		Combusted Sediment − South Dorchester Bay		
10.1	0.106	13.1	21.5	3.46
20.0[b]	0.105	9.88	41.8	3.58
20.1	0.103	13.1	35.2	3.45
40.0	0.049	5.25	74.1	3.55
40.5	0.049	4.15	57.8	3.22
46.2	0.092	21.1	47.5	3.25
51.0	0.101	4.50	76.7	3.81
52.0	0.092	2.15	82.8	3.93
59.6	0.104	13.1	60.3	3.42
96.1	0.088	21.1	73.1	3.40
102.2	0.100	15.7	58.9	3.15
195.5	0.100	15.7	73.1	3.14
199.1	0.090	21.1	92.6	3.75
		Untreated Sediment − North Quincy Bay		
11.0	0.106	9.60	32.9	3.68
19.7	0.105	9.60	50.7	3.74
41.0	0.105	9.60	68.6	3.75
59.9	0.104	9.60	73.6	3.69
		Combusted Sediment − North Quincy Bay		
10.1	0.106	9.60	22.5	3.48
20.5	0.104	9.60	53.4	3.76
39.8	0.106	9.60	64.6	3.69
60.2	0.104	9.60	87.9	4.10

[a] The error associated with the sorbent mass and volume was less than ±1%. Initial dissolved concentrations had an error of ±4%. The percent loss of pyrene and the distribution coefficient had a compounded error of ±13%, which includes reproducibility error, instrumental error, and experimental error with the oven. [b] Sediments combusted at 375 °C at WHOI using a programmable muffle furnace.

temperature. Second, based on the 365 °C, 375 °C, and 385 °C data (Table 3), the lower carbon weight percents and lower log K_d values for the sediment combusted at WHOI indicate that the cycling of the MIT oven may have caused the effective combustion temperature to be <375 °C.

Sorption to OC Fraction. The similar distribution coefficients for pyrene sorption onto untreated and combusted sediments (Figure 3a,b) demonstrated the strong contribution of BC to the overall sorption of pyrene in the original sediments. The PAH composition data and the f_{BC} values support the contention that combustion-derived solids have accumulated in these sediments. These results have several implications regarding BC as a sorbent in coastal environments.

The absorption model (eq 1), which ascribes all hydrophobic compounds' sorption to partitioning into natural organic matter (*1*, *2*), underestimated the extent of pyrene sorption at our sites. With a log K_{oc} for pyrene of 4.7 (*2*, *66*), the expected log K_d value for SDB was 2.78 ± 0.06 and for NQB was 3.19 ± 0.08. These values were significantly less than the observed values for the untreated sediments (Figure 4a,b). One argument for this discrepancy was that the chosen literature value for log K_{oc} was too low. The most renowned K_{oc}-K_{ow} correlation for PAHs was reported by Karickhoff in 1981 ($\log K_{oc} = 0.989 \log K_{ow} - 0.346$ (*2*)). The log K_{oc} for pyrene using this equation is 4.7 with a log K_{ow} of 5.1. However, several K_{oc}-K_{ow} correlations for PAHs exist in the literature. Gawlik et al. compiled most of the reported K_{oc}-K_{ow} correlations, and using these equations, the log K_{oc} for pyrene ranged from 5.0 to 3.9 with an average log K_{oc} of 4.7 (*66*). Hence, we suggest that the log K_{oc} value for pyrene is approximately 4.7.

Another argument was that the log K_{oc} for pyrene in this particular organic matter was uncharacteristically higher than most literature values. With an OC fraction of 0.012 at SDB (log K_d of 3.54) and 0.031 at NQB (log K_d of 3.72), the calculated log K_{oc} from both sites would be approximately 5.3, similar

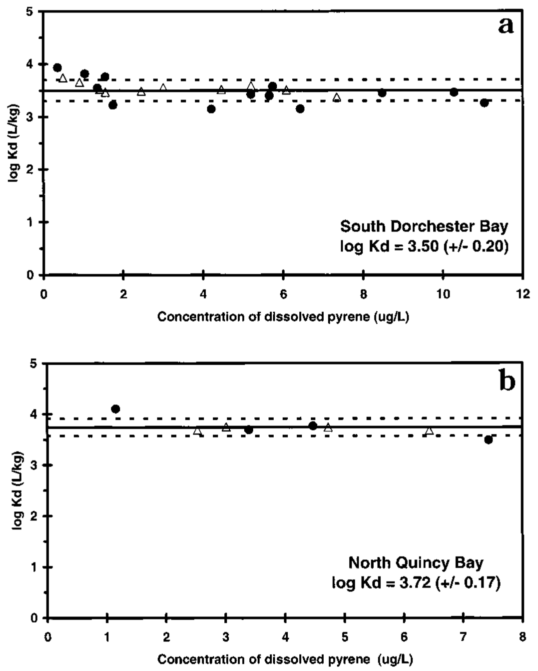

FIGURE 3. The dependence of the sediment−water distribution coefficients (L/kg$_{sed}$) on dissolved pyrene concentrations (μg/L) for Boston Harbor sediments. (a) Distribution coefficients for untreated (open triangles) and combusted (circles) sediments from SDB with a mean log K_d of 3.50 ± 0.20. (b) Distribution coefficients for untreated (open triangles) and combusted (circles) sediments from NQB with a mean log K_d of 3.72 ± 0.17. Data corresponds to experimental results listed in Table 2.

TABLE 3. Summary of Results for South Dorchester Bay Sediment Combusted at WHOI[a]

sorbent (mg)	volume (L)	initial concn (μg/L)	percent loss of dissolved pyrene	log K_d (L/kg)	fraction BC[b,c]
		365 °C Combusted Sediment at WHOI			
20.0	0.105	9.88	31.7	3.38	0.22 ± 0.03
20.0	0.105	9.88	31.8	3.39	
20.0	0.104	9.88	36.9	3.48	
		375 °C Combusted Sediment at WHOI			
20.0	0.107	9.88	18.2	3.08	0.18 ± 0.04
20.0	0.105	9.88	41.8	3.58	
20.0	0.103	9.88	30.1	3.34	
		385 °C Combusted Sediment at WHOI			
20.0	0.106	9.88	20.3	3.13	0.15 ±0.03
20.0	0.105	9.88	18.2	3.07	
20.0	0.105	9.88	24.2	3.22	

[a] The error associated with the sorbent mass and volume was less than ±1%. Initial dissolved concentrations had an error of ±4%. The percent loss of pyrene and the distribution coefficient had a compounded error of ±13%, which includes reproducibility error, instrumental error, and experimental error with the oven. [b] BC weight percent (mean ± 1σ). [c] Acetanilide carbon weight percents (mean ± 1σ) was 71.14 ± 0.02.

to reported values by Chiou et al. (*67*). However, this log K_{oc} value is greater than the pyrene log K_{ow} of 5.1. We are uncomfortable with K_{oc} values that exceed their K_{ow} values since natural organic matter is slightly hydrophilic.

While petroleum in the sediments can contribute to a larger K_{oc} value, analysis of extracted PAHs suggested that high-temperature pyrolysis was the dominant source at SDB and NQB. For example, the phenanthrene/Σmethylphenanthrenes ratio was 3 at both sites (other ratios discussed above). In addition, the fraction of extractable lipid from SDB sediments was 0.002 (personal communication from G. Ewald) corresponding to a K_d value of only 250 L/kg assuming that the distribution coefficient for octanol applies. Therefore, the lipid/oil fraction alone cannot account for the large K_d values of 3500 L/kg observed at SDB. Likewise, the fraction of extractable lipid at NQB was 0.01, which only accounts for 24% of the observed K_d value (5200 L/kg). Another sorbent, like BC, must be present in the sediment to account for the observed K_d values and the corresponding large K_{oc} values (*13*−*19*).

Sorption to BC Fraction. To accommodate additional sorption to BC, Gustafsson et al. suggested a model that described the observed distribution coefficient as a sum of two linear isotherms involving the OC fraction and the BC fraction (*10*):

$$K_d = f_{oc}K_{oc} + f_{BC}K_{BC} \tag{5}$$

This model assumed that the BC-water distribution coefficient for pyrene (K_{BC}) was independent of the dissolved concentration; however, our combusted sediment data suggested that K_{BC} is dependent on sorbate levels (Figure 3a,b). To assess whether our data suggested a dependency on the dissolved concentration, we looked at the correlation coefficients for different linear and nonlinear models. While correlation coefficients cannot prove linearity, they should increase from a linear model to a Langmuir model or a Freundlich model because the number of fitting parameters is increasing in the models from one to two. For example, for our untreated-sediment data, the R^2 value was 0.88 assuming a linear model; this correlation increased to 0.91 for the Langmuir model and continued to increase to 0.95 for the Freundlich model. In this sense, the nonlinear Freundlich model fitted our data better than a linear model. For our combusted sediment, the R^2 value was 0.72 for the linear model, decreased to 0.50 for the Langmuir model, and then increased again to 0.70 for the Freundlich model. This situation implied that correlation coefficients alone cannot distinguish between a linear or nonlinear model for the combusted sediment.

To determine if the sorption to the combusted sediment was linear, we looked at the Freundlich exponent to disprove the linear scenario (i.e., $n \pm 1\sigma \neq 1$). We calculated a Freundlich exponent of $n = 0.62 \pm 0.12$ (Figure 5) implying that sorption to the combusted sediment was nonlinear. This nonlinearity may not be surprising since sorption isotherms to activated carbon are widely reported as nonlinear (*25*−*27*). Furthermore, Bucheli and Gustafsson reported a Freundlich exponent of 0.67 for sorption of pyrene onto NIST diesel soot (*23*). Likewise, work by Ghosh et al. using a microprobe laser desorption technique to examine coal dust in Milwaukee Harbor sediments showed that PAHs resided on the external surfaces of carbonaceous material (*68*). These observations suggest that adsorption of PAHs onto BC in our combusted sediments may have a similar adsorption mechanism, and not all surface sites may exhibit equal affinities for pyrene.

While pyrene is adsorbing to the BC fraction, it is simultaneously partitioning into the thermally labile organic matter. To incorporate both of these sorption mechanisms, we modified eq 5 to yield:

$$K_d = f_{oc}K_{oc} + f_{BC}K_{BC}C_w^{\,n-1} \tag{3}$$

where the BC-normalized distribution coefficient (K_{BC}) is $10^{6.25\pm0.14}$ based on normalizing the best-fit Freundlich K_d value of $10^{3.67\pm0.08}$ ($N = 13$; Figure 5) to the measured BC fraction in SDB combusted sediment. This new model (or eq

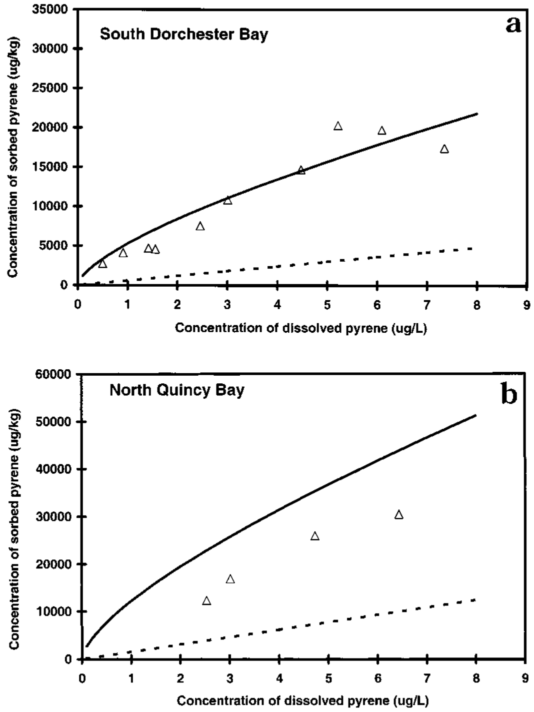

FIGURE 4. Sorbed pyrene (μg/kg$_{sed}$) vs dissolved pyrene concentrations (μg/L) deduced from (a) SDB untreated sediments (open triangles) and (b) NQB untreated sediments (open triangles). The error associated with the dissolved pyrene concentration was ±8%, which propagated to ±15% error for the sorbed concentration. Also shown are (i) the expected sorbed concentrations from $C_s = f_{oc}K_{oc}C_w$ (dashed line) and (ii) the model predicted sorbed concentrations from $f_{oc}K_{oc}\,C_w + f_{BC}K_{BC}C_w^{\,n}$ (solid line) where f_{oc} is the OC content, K_{oc}(pyrene) = $10^{4.7}$, f_{BC} is the BC content, K_{BC}(pyrene) = $10^{6.25+0.14}$, and n is 0.62 ± 0.12.

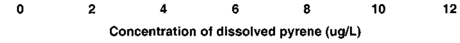

FIGURE 5. Sorbed pyrene (μg/kg$_{sed}$) vs dissolved pyrene concentrations (μg/L) deduced for SDB combusted sediment (circles; 375 °C for 24 h under air). The error associated with the dissolved pyrene concentration was ±12%, which propagated to ±22% error for the sorbed concentration. Also shown are (i) the predicted sorbed concentrations (solid line) for the best-fit Freundlich isotherm through our data with the parameters K_d(pyrene) = $10^{3.67+0.08}$ (which implies that $K_{BC} = 10^{6.25+0.14}$ with a $f_{BC} = 0.0026 \pm 0.0007$) and $n = 0.62 \pm 0.12$ and (ii) the sorbed pyrene concentration (dashed line) assuming that the BC at SDB sorbed like the diesel soot investigated by Bucheli and Gustafsson (*23*) with a $K_{BC} = 10^{6.55}$ and $n = 0.67$.

2, rewritten in terms of the sorbed concentration) was tested to predict the pyrene sorption to untreated SDB sediment. Good agreement was found between the observed and predicted sorbed pyrene concentrations (Figure 4a) using the parameters derived from our combusted sediment experiments ($n = 0.62$ and $\log K_{BC} = 6.25$), a literature value for $\log K_{oc}$ ($10^{4.7}$), and the measured f_{oc} and f_{BC} values for SDB. Since BC was a significant sorbent at this site (Figure 3a)—contributing to about 80% of the overall distribution coefficient—an isotherm through the SDB untreated sediment was also nonlinear ($n = 0.82 \pm 0.07$; Figure 4a) reflecting the presence of this BC fraction. While BC was the dominant sorbent at SDB, the OC fraction was still an important sorbent and contributed to about 20% of the overall K_d value (3500 L/kg). Nonetheless, sorption to BC may explain many reported cases of nonlinear sorption isotherms as well as cases where the $\log K_{oc}$ value exceeds the $\log K_{ow}$ value.

Sorption to NIST Soot. Our data for SDB combusted sediment fell well below the Freundlich isotherm derived by Bucheli and Gustafsson (Figure 5 (*23*)). This difference chiefly resulted from the larger distribution coefficient for NIST diesel soot ($\log K_{NIST\ BC} = 6.55$) than our environmental BC ($\log K_{BC} = 6.25 \pm 0.14$). The lower distribution coefficient for our combusted sediment, along with our C/H/N data, indicated that our near shore BC was not dominated by diesel soot. If our near shore sites contain disproportionately more of the larger BC particles, then near shore BC would have less surface area than submicron NIST diesel soot settling offshore. Consequently, lower K_{BC} values are expected on a BC-normalized mass basis. Moreover, environmental BC in the Boston Harbor is likely a combination of carbonaceous solids, conceivably each sorbing compounds, like pyrene, with different strengths. For example, carbon black from tire wear may be a big contributor to environmental BC where street runoff is important (*69*), but this graphite-like BC may not be a strong sorbent. Kim et al. predicted that the distribution coefficient for carbon black was 1.1−4.4% of the distribution coefficient for activated carbon (K_{ac}, L/kg$_{ac}$ (*70*)), and we suspect that K_{BC} approximates K_{ac} (*22*). Hence, due to variations in specific surface areas and surface chemistries, various BC types may exhibit significantly different distribution coefficients.

Application of New Sorption Model (Eq 3) at Other Boston Harbor Sites. Based on the elemental analysis of the combusted sediments at SDB and NQB and the proximity of these sites, the environmental BC at both sites may be similar (Table 1). Our model (eq 3) was then tested to predict the distribution coefficient for pyrene sorption to NQB sediments using the measured f_{oc} and f_{BC} values for NQB, a literature K_{oc} value ($10^{4.7}$), and the Freundlich exponent (0.62) and K_{BC} value ($10^{6.25}$) from SDB. While the predicted distribution coefficients were 0.1−0.3 log units above the measured values, they were within error for three of the four comparisons (Table 4). The largest overestimation of the distribution coefficient was at the lowest dissolved concentration (2.53 μg/L) where the predicted $\log K_d$ of 3.96 ± 0.14 exceeded the observed $\log K_d$ of 3.69 ± 0.05.

While extrapolation of our BC parameters from SDB to NQB may be reasonable, it is unclear how these parameters apply to other sites in the Greater Boston Harbor and lower pyrene concentrations (10−100 ng/L). McGroddy and Farrington reported $\log K_d$ values (derived from dissolved-PAH and sorbed-PAH concentrations in cores from Boston Harbor) that were unexpectedly high (*16*). In this study, the measured BC weight percents at FPC (15−17 cm depth) and SI (16−18 cm depth) were 0.84 ± 0.05% and 0.40 ± 0.12%, respectively. Both of these subsections were deep enough in the core, so bioturbation and pore water flushing did not affect PAH equilibrium with the sediment. At FPC, the sorbed and dissolved pyrene data indicated a $\log K_d$ of 4.32 ± 0.15 with a dissolved pyrene concentrations near 0.4 μg/L (Table 4 (*71*)). This value measured under field conditions compared very well to a predicted $\log K_d$ of 4.39 ± 0.18 using eq 3. Likewise, at SI with a dissolved pyrene concentration of 0.06 μg/L, our model predicted a $\log K_d$ value of 4.34 ± 0.18, which was within error of the observed $\log K_d$ value of 4.55 ± 0.15 (Table 4). The agreement between the predicted and measured distribution coefficients suggests (1) similar BC matrices occur around Boston Harbor and (2) our approach is reasonable for predicting $\log K_d$ values at environmental concentrations.

TABLE 4. Measured versus Predicted Distribution Coefficients for North Quincy Bay Untreated Sediment, McGroddy Fort Point Channel (15−17 cm), and McGroddy Spectacle Island (16−18 cm)

dissolved pyrene (μg/L)^a	measd $\log K_d$ (L/kg$_{sed}$)^b	predicted $\log K_d$ (L/kg$_{sed}$)^c
	North Quincy Bay	
6.44	3.68 ± 0.05	3.83 ± 0.14
4.73	3.74 ± 0.05	3.87 ± 0.14
3.02	3.75 ± 0.05	3.93 ± 0.14
2.53	3.69 ± 0.05	3.96 ± 0.14
	McGroddy Fort Point Channel	
0.4	4.32 ± 0.15	4.39 ± 0.18
	McGroddy Spectacle Island	
0.06	4.55 ± 0.15	4.34 ± 0.18

[a] Measured dissolved pyrene concentration for the untreated sediment at NQB is the same data as Table 2, and data for Fort Point Channel and Spectacle Island are from McGroddy (*71*). [b] Measured distribution coefficient (mean $\pm 1\sigma$) for the untreated sediment at NQB is same data as Table 2, and data for Fort Point Channel and Spectacle Island are from McGroddy (*71*). [c] Predicted distribution coefficient (mean $\pm 1\sigma$) with the new model (eq 3) assuming that $\log K_{oc} = 4.7$, $\log K_{BC} = 6.25 \pm 0.14$, and $n = 0.62 \pm 0.12$.

Implications. Our results have several implications to the importance of BC as a sorbent in soils and sediments. First, the sorption of other PAH-like compounds onto BC may explain reported nonlinear isotherms (*28*−*32*) and unexpectedly high K_{oc} values (*72*). Second, since BC is ubiquitous in the environment and has been disseminated over geological time (*51*), a large percentage of the aromatic content observed with ^{13}C NMR (*67*) in the soil and sediment organic matter may be due to the presence of BC. Therefore, we support the institution of a new procedure to quantify the BC fraction and to identify the various BC components (i.e. char, fly ash, and soot) in natural solids before they are tested as sorbents. This new procedure would also apply to atmospheric particles, which are known to contain BC (often referred to as elemental carbon (EC) in atmospheric literature (*73*, *74*)).

In addition, BC in sediments and soils will affect the desorption rates of planar organic compounds such as PAHs, and conceivably coplanar PCB congeners, pesticide derivatives such as DDE, and polychlorinated dibenzodioxins and furans. Based on our observed sorption kinetics and equilibrium constants, the equilibration time in aquatic environments having a low BC-to-water ratio could approach months (*75*). Last, our data suggest that we should expect very different bioaccumulation and biodegradation for sediments that contain (1) a significant BC fraction versus sediments that do not and (2) BC-sorbed compounds such as PAHs. The BC fraction in SDB and NQB sediments would lower the chemical availability of PAHs by 4−6 times that expected from $f_{oc}K_{oc}$ alone, and this difference is similar to the “discrepancy” in Biota-Sediment Accumulation Factors reported widely between PCBs and PAHs (*76*).

Acknowledgments

This work was supported by NSF Grant No. BES-9800485 and project number RC-70 of the MIT Sea Grant College Program under a federal grant number NA86RG0074 from the National Sea Grant College Program, National Oceanic and Atmospheric Administration, U.S. Department of Commerce. We thank Goran Ewald, John MacFarlane, and John Farrington for sediment collection; John MacFarlane, Jed Goldstone, and Christopher Swartz for assistance in the lab; and Ana Lima for assistance in combusting sediments at WHOI. We also thank Tim Eglinton, Chris Reddy, Jean Whelan, Richard Bopp, and Greg Noonan for guidance and helpful discussions.

Literature Cited

(1) Chiou, C. T.; Peters, L. J.; Freed, V. H. *Science* **1979**, *206*, 831−832.
(2) Karickhoff, S. W. *Chemosphere* **1981**, *10*, 833−846.
(3) Weber, W. J.; McGinley, P. M.; Katz, L. E. *Environ. Sci. Technol.* **1992**, *26*. 1955−1962.
(4) Steinberg, S. M.; Pignatello, J. J.; Sawhney, B. I. *Environ. Sci. Technol.* **1987**, *21*, 1201−1208.
(5) Scribner, S. L.; Benzing, T. R.; Sun, S.; Boyd, S. A. *J. Environ. Qual.* **1992**, *21*, 115−120.
(6) Keil, R. G.; Montlucon, D. B.; Prahl, F. G.; Hedges, J. L. *Nature* **1994**, *370*, 549−552.
(7) Tang, J.; Garcia, R.; Holden, K. M. L.; Mitchell, S. C.; Pis, J. J. *Environ. Sci. Technol.* **1998**, *32*, 3586−3590.
(8) Alexander, M. *Environ. Sci. Technol.* **2000**, *34*, 4259−4265.
(9) Grathwohl, P. *Environ. Sci. Technol.* **1990**, *24*, 1687−1693.
(10) Gustafsson, Ö.; Haghseta, F.; Chan, C.; MacFarlane, J.; Gschwend, P. M. *Environ. Sci. Technol.* **1997**, *31*, 203−209.
(11) Luthy, R. G.; Aiken, G. R.; Brusseau, M. L.; Cunningham, S. D.; Gschwend, P. M.; Pignatello, J. J.; Reinhard, M.; Triana, S. J.; Weber, W.; Westall, J. C. *Environ. Sci. Technol.* **1997**, *31*, 3341−3347.
(12) Lamoureux, E. M.; Brownawell, B. J. *Environ. Toxicol. Chem.* **1999**, *18*, 1733−1741.
(13) Prahl, F. G.; Carpenter, R. *Geochim. Cosmochim. Acta* **1983**, *47*, 1013−1023.
(14) Socha, S. B.; Carpenter, R. *Geochim. Cosmochim. Acta* **1987**, *51*, 1273−1284.
(15) Readman, J. W.; Mantoura, R. F. C.; Rhead, M. M. *Sci. Total Environ.* **1987**, *66*, 73−94.
(16) McGroddy, S. E.; Farrington, J. W. *Environ. Sci. Technol.* **1995**, *29*, 1542−1550.
(17) Simpson, C. D.; Mosi, A. A.; Cullen, W. R.; Reimer, R. J. *Sci. Total Environ.* **1996**, *181*, 265−278.
(18) Zhou, J. L.; Fileman, T. W.; Evans, S.; Donkin, P.; Readman, J. W.; Mantoura, R. F. C.; Rowland, S. *Sci. Total Environ.* **1999**, *244*, 305−321.
(19) Jonker, M. T. O.; Smedes, F. *Environ. Sci. Technol.* **2000**, *34*, 1620−1626.
(20) Youngblood, W. W.; Blumer, M. *Geochim. Cosmochim. Acta* **1975**, *39*, 1303−1314.
(21) Gschwend, P. M.; Hites, R. A. *Geochim. Cosmochim. Acta* **1981**, *43*, 2359−2367.
(22) Gustafsson, Ö.; Gschwend, P. M. In *Molecular Markers in Environmental Geochemistry*; Eganhouses, R., Ed.; ACS Symposium Series; American Chemical Society: Washington, DC, 1997; pp 365−381.
(23) Bucheli, T. D.; Gustafsson, Ö. *Environ. Sci. Technol.* **2000**, *34*, 5144−5151.
(24) Kubicki, J. D.; Apitz, S. E. *Org. Geochem.* **1999**, *30*, 911−927.
(25) Crittenden, J. C.; Luft, P.; Hand, D. W.; Oravitz, J. L.; Loper, S. W.; Art, M. *Environ. Sci. Technol.* **1985**, *19*, 1037−1043.
(26) Blum, D. J. W.; Suffet, I. H.; Duguet, J. P. *Water Res.* **1994**, *28*, 687−699.
(27) Karanfil, T.; Kilduff, J. E. *Environ. Sci. Technol.* **1999**, *33*, 3217−3224.
(28) Chiou, C. T.; Kile, D. E. *Environ. Sci. Technol.* **1998**, *32*, 338−343.
(29) Xia, G. S.; Ball, W. P. *Environ. Sci. Technol.* **1999**, *33*, 262−269.
(30) Kleineidam, S.; Rugner, H.; Ligouis, B.; Grathwohl, P. *Environ. Sci. Technol.* **1999**, *33*, 1637−1644.
(31) Karapanagioti, H. K.; Kleineidam, S.; Sabatini, D.; Grathwohl, P.; Ligouis, B. *Environ. Sci. Technol.* **2000**, *34*, 406−414.
(32) Xia, G. S.; Pignatello, J. J. *Environ. Sci. Technol.* **2001**, *35*, 84−94.
(33) Shiaris, M. P.; Jambard-Sweet, D. *Mar. Pollut. Bull.* **1986**, *17*, 469−472.
(34) Gardner, G. R.; Pruell, R. J. *Mar. Environ. Res.* **1989**, *28*, 393−397.
(35) Gustafsson, Ö.; Bucheli, T. D.; Kukulska, Z.; Andersson, M.; Largeau, C.; Rouzaud, J.; Reddy, C. M.; Eglinton, T. I. *Global Biogeochem. Cycles* Submitted for publication.
(36) Eiroa, A. A.; Blanco, V.; Mahia, P. L.; Lorenzo, S. M.; Rodriguez, D. P. *Analyst* **1998**, *123*, 2113−2117.
(37) Harris, D. C. In *Quantitative Chemical Analysis*, 4th ed.; WH Freeman and Company: New York, 1995.
(38) Gauthier, T. D.; Shane, E. C.; Guerin, W. F.; Seltz, W. R.; Grant, C. L. *Environ. Sci. Technol.* **1986**, *20*, 1162−1166.
(39) Backhus, D. A.; Gschwend, P. M. *Environ. Sci. Technol.* **1990**, *24*, 1214−1222.
(40) Auger, R. L.; Jacobson, A. M.; Domach, M. M. *Environ. Sci. Technol.* **1995**, *29*, 1273−1278.
(41) Budzinski, H.; Jones, I.; Bellocq, J.; Pierard, C.; Garrigues, P. *Marine Chem.* **1997**, *58*, 85−97.
(42) Garrigues, P.; Parlanti, E.; Radk, M.; Bellocq, J.; Willsch, H.; Ewald, M. *J. Chromatogr.* **1987**, *395*, 217−228.
(43) Benner, B. A.; Gordon, G. E.; Wise, S. A. *Environ. Sci. Technol.* **1989**, *23*, 1269−1278.
(44) Benner, B. A.; Wise, S. A.; Currie, L. A.; Klouda, G. A.; Klinedinst, D. B.; Zweidinger, R. B.; Stevens, R. K.; Lewis, C. W. *Environ. Sci. Technol.* **1995**, *29*, 2382−2389.
(45) Windsor, J. G.; Hites, R. A. *Geochim. Cosmochim. Acta* **1979**, *43*, 27−33.
(46) Miguel, A. M.; Kirchstetter, T. W.; Harley, R. A. *Environ. Sci. Technol.* **1998**, *32*, 450−455.
(47) Gustafsson, Ö.; Gschwend, P. M. *Geochim. Cosmochim. Acta* **1998**, *62*, 465−472.
(48) Schmidt, M. W. I.; Noack, A. G. *Global Biogeocem. Cycles.* **2000**, *14*, 777−793.
(49) Middelburg, J. J.; Nieuwenhuize, J.; Breugel, P. *Mar. Chem.* **1999**, *65*, 245−252.
(50) Medalia, A. I.; Rivin, D. *Carbon* **1982**, *20*, 481−492.
(51) Goldberg, E. B. In *Black Carbon in the Environment: Properties and Distribution;* A Wiley-Interscience Publication, John Wiley & Sons: New York, 1985; pp 1−198.
(52) Kulbusch, T. A. J.; Crutzen, P. J. *Global Biogeochem. Cycles* **1995**, *9*, 491−501.
(53) Rockne, K. J.; Taghon, G. L.; Kosson, D. S. *Chemosphere* **2000**, *41*, 1125−1135.
(54) Sumam, D. O.; Kulbusch, T. A. J.; Lim, B. In *Sediment Records of Biomass Burning and Global Change;* Clarks, J. S., Ed.; NATO ASI Series; 1994; pp 271−293.
(55) Ruttenberg, K. C.; Goni, M. A. *Mar. Geol.* **1997**, *139*, 123−145.
(56) Akhter, M. S.; Chughtal, A. R.; Smith, D. M. *Appl. Spectrosc.* **1985**, *39*, 143−153.
(57) Harris, S. J.; Weine, A. M. *Combust. Sci. Technol.* **1983**, *31*, 155−167.
(58) Lahaye, J. *Polym. Degrad. Stabil.* **1990**, *30*, 111−121.
(59) Frenklach, M. In *Twenty-sixth Symposium (International) on Combustion*; The Combustion Institute: Pittsburgh, PA, 1996; pp 2285−2293.
(60) Handa, T.; Yamauchi, T.; Sawai, K.; Yamamura, T.; Koseki, Y.; Ishii, T. *Environ. Sci. Technol.* **1984**, *18*, 895−902.
(61) Dimashki, M.; Harrad, S.; Harrsion, R. M. *Atmos. Environ.* **2000**, *34*, 2459−2469.
(62) Kozin, I. S.; Larsen, O. F. A.; Voogt, P. d.; Gooijer, C.; Velthorst, N. H. *Anal. Chim. Acta* **1997**, *354*, 181−187.
(63) Chin, Y.; Gschwend, P. M. *Environ. Sci. Technol.* **1992**, *26*, 1621−1626.
(64) MacDonald, B. C.; Lvin, S. J.; Patterson, H. *Anal. Chim. Acta* **1997**, *338*, 155−162.
(65) Mitra, S.; Dickhut, R. M. *Environ. Toxicol. Chem.* **1999**, *18*, 1144−1148.
(66) Gawlik, B. M.; Sotiriou, N.; Feicht, E. A.; Schulte-Hostede, S.; Kettrup, A. *Chemosphere* **1997**, *34*, 2525−2551.
(67) Chiou, C. T.; McGroddy, S. E.; Kile, D. E. *Environ. Sci. Technol.* **1998**, *32*, 264−269.
(68) Ghosh, U.; Gillette, S.; Luthy, R. G.; Zare, R. N. *Environ. Sci. Technol.* **2000**, *34*, 1729−1736.
(69) Reddy, C. M.; Quinn, J. G. *Environ. Sci. Technol.* **1997**, *31*, 2847−2853.
(70) Kim, J. Y.; Park, J. K.; Edil, T. B. *J. Environ. Eng.* **1997**, *123*, 827−835.
(71) McGroddy, S. E. Ph.D. Thesis, University of Massachusetts at Boston: Boston, 1993; pp 1−255.
(72) Bucheli, T. D.; Gustafsson, Ö. *Environ. Toxicol. Chem.* **2001**, *20*, 1450−1456.

(73) Hildemann, L. M.; Markowski, G. R.; Cass, G. R. *Environ. Sci. Technol.* **1991**, *25*, 744−759.

(74) Venkataraman, C.; Friedlander, S. K. *Environ. Sci. Technol.* **1994**, *28*, 563−572.

(75) Wu, S. C.; Gschwend, P. M. *Environ. Sci. Technol.* **1986**, *20*, 717−725.

(76) Tracey, G. A.; Hansen, D. J. *Arch. Environ. Contam. Toxicol.* **1996**, *30*, 467−475.

Received for review May 8, 2001. Revised manuscript received October 10, 2001. Accepted October 22, 2001.

ES010953C